A new series of optoelectronic nanocomposites: CMI-1 mesoporous core/ZnS shell

Piret, François; Bouvy, Claire; Marine, Wladimir; Su, Bao-Lian

[Link to publication](#)

Citation for pulished version (HARVARD):
Piret, F, Bouvy, C, Marine, W & Su, B-L 2007, 'A new series of optoelectronic nanocomposites: CMI-1 mesoporous core/ZnS shell', *Chemical Physics Letters*, vol. 441, pp. 83-87.

A new series of optoelectronic nanocomposites: CMI-1 mesoporous core/ZnS shell

F. Piret [a,1], C. Bouvy [a,1], W. Marine [b], B.L. Su [a,*]

[a] *Laboratoire de Chimie des Matériaux Inorganiques (CMI), The University of Namur (FUNDP), Rue de Bruxelles 61, B-5000 Namur, Belgium*
[b] *CRMCN, UPR 7251 CNRS, Faculté des Sciences de Luminy, Université de la Méditerranée Aix Marseille II, F-13288 Marseille, Cedex 9, France*

Abstract

The conception of a totally new optoelectronic composite with a highly organized mesoporous silica core and a uniform ZnS shell (200 nm in thickness) with new optical properties is reported. The starting CMI-1 material was firstly functionalized with ethylenediamine groups and then the growth of the ZnS shell was targeted by the immersion of the functionalized CMI-1 material in a $Zn(CH_3COO)_2$ solution followed by a reaction with sodium sulfide. The new optoelectronic nanocomposite has been characterized by a series of techniques such as SEM, TEM and nitrogen adsorption–desorption. The optical properties of the new nanocomposite have been evaluated by photoluminescent spectroscopy. No quantum size effect has been observed due to the large size aggregates in ZnS later.
© 2007 Elsevier B.V. All rights reserved.

1. Introduction

The design of new composites is a fascinating field of research in chemistry, physics and biology. In particular, semiconductor-based composites are attractive materials for a variety of optoelectronic applications including light-emitting devices [1] and optical switches [2]. These nanocomposites can also be used in solar photovoltaic systems [3] and as chemical/biological sensors [4]. Such broad range and diversity in application possibilities give material scientists a practical incentive to make greater efforts towards the design of new semiconductor-based (nano)composites.

Recently, core/shell composites are attracting the increasing attention. These materials can be synthesized either by a direct surface reaction/precipitation or by the layer-by-layer (LBL) approaches. Various core/shell materials have been prepared such as silica/polymer [5], metal/ metal [6], metal/semiconductor [7] or semiconductor/semiconductor [8]. Semiconductor-based core/shell (nano-)composites are particularly interesting due to their advanced applications in electronics, photonics and photocatalysis nanotechnology [9,10]. Silica coated luminescent semiconductor CdS nanocrystals have thus been synthesized and showed good photocatalytic activity and optoelectronic performance [11]. The silica shell could enhance photochemical stability and increase the quantum yield of the nanocrystalline core. However, in spite of the optical transparency of silica, the electrical isolation of silica limits the application of semiconductor core/silica shell nanocomposites. The nanocomposite formed by silica core and semiconductor shell renders, on the other hand, the semiconductor accessible to an electron beam.

Zinc sulfide is a very important II–IV semiconductor compound with a large direct band gap for bulk material (3.66 eV at RT). It is used as a key material in many optoelectronic applications such as light-emitting diodes [12], cathode-ray tubes [13], thin film electroluminescence [14] and window layers in photovoltaic cells [15].

Very recently, a series of optoelectronic nanocomposites have been prepared by the incoperation of ZnS and ZnO

---

* Corresponding author. Fax: +32 81 72 54 14.
E-mail address: bao-lian.su@fundp.ac.be (B.L. Su).
[1] FRIA fellow (Fonds National de la Recherche Scientifique, 5 rue d'Egmont, 1000 Bruxelles, Belgium).

nanoparticles in the channels of mesoporous silica CMI-1 materials [16,17]. By tuning the pore size of mesoporous matrices, the growth of ZnS and ZnO crystals inside the mesochannels can be limited to pore size range and thus semiconductor nanoparticle size can be well adjusted. The nanocomposites obtained showed very interesting photoluminescent properties and a quantum size effect by the significant shift of the photoluminescent emission band of ZnS and ZnO towards high energy level. This is of great importance in the design of short wavelength lasers, blue-light-emitting diodes and UV detection. However, due to the dispersion of nanoparticles in the whole micrometric particles of mesoporous silicas, the polydispersity of nanoparticles in size and the location of large particles at the outer surface of mesoporous silicas, the photoluminescent intensity needs to be enhanced and new methods have to be developed to get the homogeneity of nanoparticles inside the mesochannels.

The aim of this study is the design of a new family of a core/shell optoelectronic composite based on silica mesoporous material and ZnS. A layer-by-layer method was performed in the preparation of the mesoporous silica core/ZnS shell nanocomposite. Mesoporous silica CMI-1 materials have been demonstrated to be ideal candidates as hosts for this new family of silica core/ZnS shell [16–18]. For an easy incoperation of ZnS particles in the mesochannels, the mesoporous CMI-1 material was firstly functionalized by anchoring ethylendiamine groups that are able to chelate Zn^{2+} ions. The ZnS shell was produced by a two step method. Firstly, the incorporation of zinc ions only at the entrance of the channels of mesoporous silica CMI-1 by the 'incipient wetness procedure' [16,19] was achieved, conducting to a shell of Zn^{2+} ions with high concentration. This was followed by the reaction of the Zn^{2+} ion shell with sulfide ions in aqueous solution called 'combination' step. This new composite has been characterized by a series of techniques such as SEM, TEM, N_2 adsorption–desorption and the optical properties have been studied by using photoluminescent spectroscopy.

2. Experimental

The highly ordered mesoporous material CMI-1 was prepared using cetyldecaoxyethylene alkyl ether $C_{16}(EO)_{10}$ as surfactant to direct the mesophase formation with the procedure reported in the literature [20]. The final product was recovered after ethanol extraction using Soxhlet apparatus for a period of 30 h and then calcined at 500 °C for 18 h to remove all the surfactant and impurities. The elimination of surfactant molecules by solvent extraction can avoid the generation of structural defects during calcination. We also found that the mesoporous materials synthesized by using neutral surfactant molecules contain less structural defects. This is quite important for the conception of optoelectronic materials [16–18]. The functionalization of mesoporous silica CMI-1 was carried out as described elsewhere in the literature [16].

The core/shell nanocomposite was synthesized by a two steps method described as follows: (a) 0.5 g of the surface-modified CMI-1 was suspended in 20.0 mL of a H_2O/CH_3CH_2OH (4:1) mixture containing $Zn(CH_3COO)_2 \cdot 2H_2O$ (0.1 M). After an hour of stirring at room temperature, centrifugation was used to recover the powder. (b) The CMI-1 material was added to an aqueous solution of sodium sulfide (0.1 M, 20.0 mL). The reaction was performed at room temperature for 12 h.

The TEM micrographs were taken with a 100 kV Philips Technaï microscope. Sample powders were embedded in an epoxy resin and then sectionned with an ultramicrotome. The morphologies of the samples were investigated by a Philips XL-20 scanning electron microscope (SEM) with conventional sample preparation and imaging techniques. Nitrogen adsorption–desorption isotherms were obtained at −196 °C over a wide relative pressure range from 0.01 to 0.995 with a volumetric adsorption analyzer Tristar 3000 manufactured by Micromeritics. Samples were previously degassed under vacuum for several hours at 320 °C before nitrogen adsorption measurements. The average pore diameter and the pore size distribution were determined by the BJH (Barret, Joyner, Halenda) method [21]. Photoluminescence studies were performed using a 254 nm light emission from a Hg lamp.

3. Results and discussion

The CMI-1 material has been synthesized, calcined and further surface-functionalized with ethylendiamine groups. By the control of the synthesis conditions, the morphology of mesoporous silicas can be tailored [20,22–25]. Fig. 1 shows the SEM and TEM pictures of mesoporous silica CMI-1 material. Well defined spherical particles with uniform size of 3–5 μm are obtained (Fig. 1a). It should be indicated that some particles are sticked together to give the aggregates. The spherical morphology with several micrometer in size is one of typical morphologies of mesoporous silica CMI-1 materials. The TEM picture confirms the highly ordered arrangement of mesochannels. Nitrogen adsorption–desorption isotherms of functionalized CMI-1 material remains type IV (Fig. 2Ab), characteristic of mesoporous materials. The surface area of this functionalized material is still relatively high up to 624 cm^2/g although this value is lower than that of the starting CMI-1 material which has a surface area higher than 1000 m^2/g. A very narrow and symmetrical pore size distribution centred at 3.5 nm determined by using BJH method with the adsorption branch of the isotherms is obtained, showing that after the functionalization, the mesoporosity and high organization of the mesochannels remain unchanged.

The mesoporous material was immersed in a zinc acetate solution. Owing to the stirring, the ions will diffuse inside the mesoporous channels. This method is usually referred as the incipient wetness. However, by the functionalization of amine groups, the impregnation of Zn^{2+} ions can occur only at the entrance of the amine groups functionalized
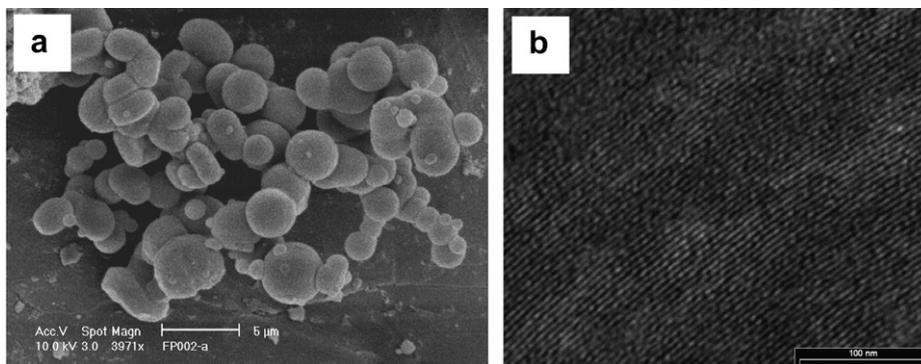
Fig. 1. SEM micrograph (a) and TEM micrograph (b) of mesoporous CMI-1 material.
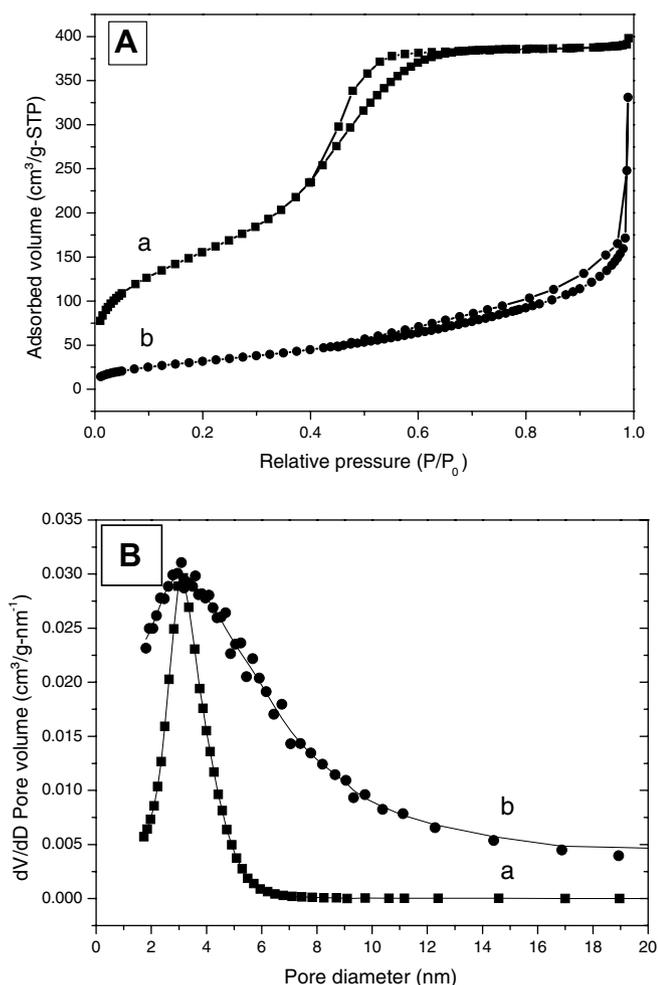

Fig. 2. The nitrogen adsorption–desorption isotherms (A) and BJH pore size distribution (B) of the CMI-1 material (a) and the core–shell composite (b).

channels of mesoporous silica, at least the most part of Zn^{2+} ions impregnated will locate at the entrance of the mesochannels. Sodium sulfide has been then introduced. The whole reaction can be represented by

$$Zn(CH_3COO)_2 + Na_2S \rightarrow ZnS + 2CH_3COONa.$$
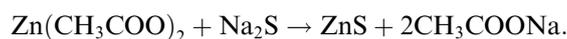
Due to the location of the most part of Zn^{2+} ions, this reaction can occur only at the entrance of the mesochannels. A layer (shell) of ZnS can thus be formed. This method can be expected to give a very homogeneous thickness layer.

Fig. 3 shows SEM and TEM pictures of the CMI-1 core/ ZnS nanocomposite. The particles are still spherical while the size is slightly enlarged and the surface of the core/shell nanocomposite particles are rougher due to the zinc sulfide shell. The SEM result shows that the CMI-1 particles were not destroyed by the synthesis of the ZnS shell. The TEM micrographs of the CMI-1 core/ZnS shell nanocomposite show an abrupt core/shell transition by the change in contrast (Fig. 3B, C). The darker shell is certainly composed of ZnS. For each particle, a homogeneous zinc sulfide shell with 200 nm in thickness surrounding a mesoporous silica core has been observed (Fig. 3B, C). The parallel channels of 3–4 nm in size can be clearly visualized (Fig. 3D). The high organization of mesochannels remains unchanged even after the formation of ZnS shell. These results show that the synthesis of the core–shell composite is highly efficient.

An important change in the nitrogen adsorption and desorption isotherms of core/shell nanocomposite is revealed. The isotherms of CMI-1 core/ZnS shell nanocomposite are more or less of type II with a very narrow hysteresis loop. At the very low relative pressure, very low adsorption quantity of N_2 was observed, giving a very low surface area. A broad pore size distribution curve still centred at 3 nm was obtained. All these results from N_2 adsorption–desorption illustrate that due to the formation of ZnS nanoparticles at the entrance of the mesochannels of mesoporous silica microspheres, the accessibility of N_2 molecules to the internal mesochannels is largely reduced, indicating the blockage of the pores by ZnS particles. The TEM picture showed the intact highly organized mesostructure and mesoporous systems. Such nanocomposite formed by a uniform ZnS shell coated on a highly organized and optically transparent mesostructured silica core should be very promising to develop new photoluminescent properties and new efficient photocatalysts.

Fig. 4a, b shows the photoluminescence (PL) spectra of CMI-1 and CMI-1 core/ZnS shell nanocomposite,
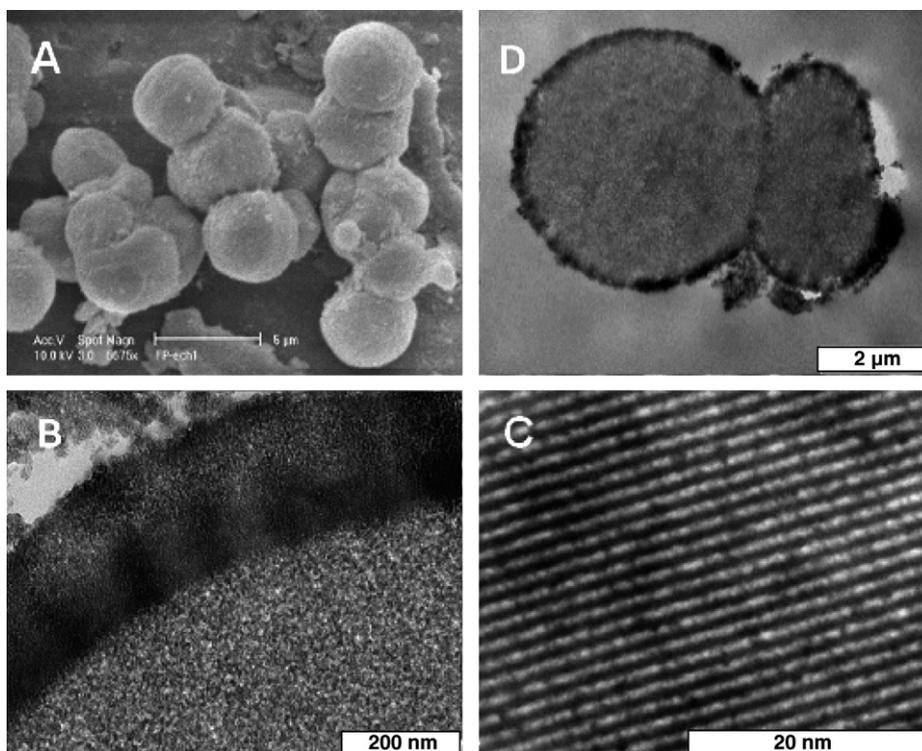
Fig. 3. SEM micrograph (A) and TEM micrographs (B–D) of CMI-1/ZnS core/shell composite.
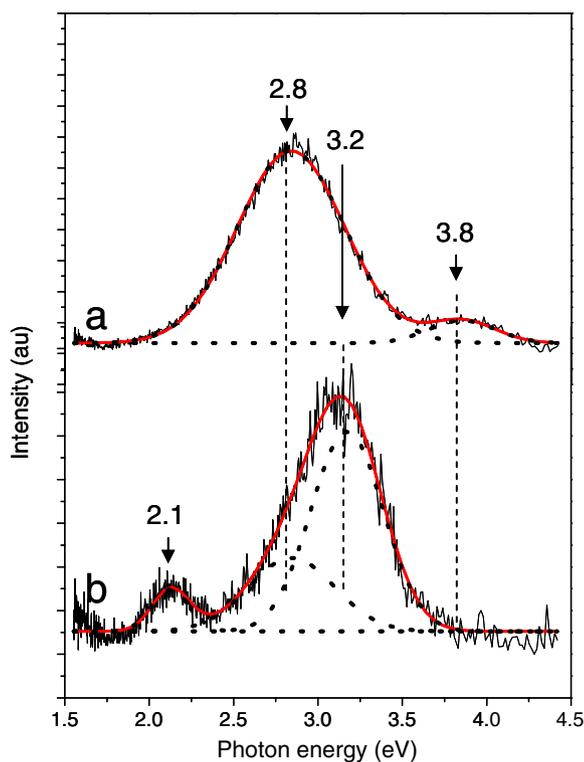

Fig. 4. Photoluminescence spectra of (a) CMI-1 Material and (b) CMI-1/ZnS core/shell composite.

mesoporous materials are still badly understood in spite of many studies [18,26–32]. Two phenomenons are complicating the extensive study. Firstly the optical properties of each kind of mesoporous materials could be different (due to the preparation conditions) and on the other hand, an unexpected shift of the emission band can be observed when employing various excitation energies [26–31].

The optical properties of mesoporous silicas are often correlated with those of amorphous silica. In an ideal silica lattice, only Si–O bonds are present and the band gap is approximately 9 eV. An electron paramagnetic resonance (EPR) study of this material revealed four kinds of structural defects which introduce electronic states into the band gap: peroxyl radicals labelled as E' centers, non-bridging oxygen holes, labelled as NBOH centres and two kinds of silanol associated defects. Each of these defect sites has a characteristic photoluminescence when excited with high photon energy ($h\nu > 3.5$ eV).

Two large emissions centred at around 2.8 and 3.8 eV were observed in the PL spectrum of the CMI-1 silica material (Fig. 4a). On the basis of our recent study, these two emission bands at 2.8 and 3.8 eV could result from the defect sites such as E' centers ($\equiv$Si·) and ($\equiv$Si–O$_2'$) type, respectively. Both are generated from the same origin: silanol groups [18]. The PL spectrum of the CMI-1 core/ZnS shell nanocomposite (Fig. 4b) revealed the disappearance of the emission band at 3.8 eV, a new emission centred around 2.1 eV and a large and asymmetric band in the range of 2.5–3.8 eV. The disappearance of the emission band at 3.8 eV was previously reported and is due to the

respectively. The aim of this Letter is not to give an overview of all hypotheses concerning the photoluminescence of silica materials. The photoluminescent properties of

interaction of ZnS semiconductor with the silanol defects which can switch off the PL properties of these defects. The new emission band at 2.1 eV was often observed in an amorphous silica and can be attributed to structural non-bridging oxygen hole centers (NBOHC) inside the silica network. These defects have been created by the introduction of the ZnS shell on the outer surface of silica particles although this kind of defects is never observed in mesoporous CMI-1 materials. We found that the functionalization step did not generate this kind of defects. The impregnation procedures of CMI-1 material in Zn acetate and then in sodium sulfide solutions could be responsible for the creation of these new defects. The large asymmetric emission band in the range of 2.5–3.8 eV can be decomposed using Gaussian function to two contributions, one with low intensity at 2.8 eV and another with high intensity at 3.2 eV. The first one has been observed in the starting CMI-1 material and is due to E' centers ($\equiv$Si$\cdot$) [18]. The second one can arise from the recombination of excitons in the ZnS shell. This emission has already been observed at 3.25 eV by our group and corresponds to the PL emission of bulky ZnS [16,17,19]. No band shift to high energy can be observed, indicating the absence of the Quantum size effect which is often observed in our nanocomposites made by the incoperation of ZnO or ZnS nanoparticles in mesochannels of CMI-1 materials. This suggests that due to the formation of a ZnS shell, ZnS nanoparticles formed initially are gathered together to form larger aggregates with too large size to generate a quantum size effect. However, the high PL emission intensity generated from ZnS shell can be further explored to develop the optoelectronic properties and photocatalytic activity.

4. Conclusions

A new preparation method conducting to a new CMI-1 core/ZnS shell optoelectronic nanocomposite was developed. The ZnS shell is quite well uniform with a thickness of 200 nm and the core preserves its highly organized mesoporous structure with well ordered mesochannels. Due to the special core/shell structure, some new optical properties were revealed. However, due to the aggregation of ZnS particles to form the shell, no quantum size effect can be observed. Not only the photoluminescene properties have to be further explored, but also the photocatalytic activity of such core/shell system has to be evaluated since such structure can give a maximum contact surface to reagents.

Acknowledgements

References

[1] J. Bao, M.A. Zimmler, F. Capasso, X. Wang, Z.F. Ren, Nanoletter 6 (2006) 1719.
[2] M. Shim, C. Wang, P. Guyot-Sionnest, J. Phys. Chem. B. 105 (2001) 2369.
[3] B. Levy, W. Liu, S.E. Gilbert, J. Phys. Chem. B 101 (1997) 1810.
[4] P.T. Snee, R.C. Somers, G. Nair, J.P. Zimmer, M.G. Bawendi, D.G. Nocera, J. Am. Chem. Soc. 128 (2006) 13320.
[5] X. Ding, J. Zhao, Y. Liu, H. Zhang, Z. Wang, Mater. Lett. 58 (2004) 3126.
[6] N.S. Sobal, U. Ebels, H. Möhwald, M. Giersig, J. Phys. Chem. B 107 (2003) 7351.
[7] P.V. Kamat, M. Flumiani, A. Dawson, Colloids Surf. A 202 (2002) 269.
[8] A.R. Loukanov, C.D. Dushkin, K.I. Papazova, A.V. Kirov, M.V. Abrashev, E. Adachi, Colloids Surf. A 245 (2004) 9.
[9] D. Yu, J. An, Colloids Surf. A 237 (2004) 87.
[10] D. Gerion, F. Pinaud, S.C. Williams, W.J. Parak, D. Zanchet, S. Weiss, A.P. Alivisatos, J. Phys. Chem. B 105 (2001) 8861.
[11] F. Teng, Z. Tian, G. Xiong, Z. Xu, Catal. Today 93–95 (2004) 651.
[12] T. Yamamoto, S. Kishimoto, S. Iida, Phys. B 308–310 (2001) 916.
[13] M. Bredol, J. Merikhi, J. Mater. Sci. 33 (1998) 471.
[14] Y. Kavanagh, M.J. Alam, D.C. Cameron, Thin Solid Films 447–448 (2004) 85.
[15] L.X. Shao, K.H. Chang, H.L. Hwang, Appl. Surf. Sci. 212–213 (2003) 305.
[16] C. Bouvy, F. Piret, W. Marine, B.L. Su, Chem. Phys. Lett. 433 (2007) 350.
[17] C. Bouvy, W. Marine, B.L. Su, Chem. Phys. Lett. 438 (2007) 67.
[18] C. Bouvy, W. Marine, R. Sporken, B.L. Su, Chem. Phys. Lett. 420 (2006) 225.
[19] C. Bouvy, W. Marine, B.L. Su, Chem. Phys. Lett. 428 (2006) 312.
[20] J.L. Blin, A. Leonard, B.L. Su, Chem. Mater. 13 (2001) 3542.
[21] E.P. Barret, L.G. Joyner, P.P. Halenda, J. Am. Chem. Soc. 73 (1951) 373.
[22] J.L. Blin, A. Becue, B. Pauwels, G. Van Tendeloo, B.L. Su, Micropor. Mesopor. Mater. 44–45 (2001) 41.
[23] J.L. Blin, A. Leonard, B.L. Su, J. Phys. Chem. B 105 (2001) 6070.
[24] G. Herrier, J.L. Blin, B.L. Su, Langmuir 17 (2001) 4422.
[25] B.L. Su, A. Leonard, Z.Y. Yuan, C.R. Chimie 8 (2005) 713.
[26] H. Nishikawa, T. Shiroyama, R. Nakamura, Y. Ohki, K. Nagasawa, Y. Hama, Phys. Rev. B 45 (1992) 586.
[27] K.S. Seol, A. Ieki, Y. Ohki, H. Nishikawa, M. Tachimori, J. Appl. Phys. 79 (1996) 412.
[28] R. Tohmon, H. Mizuno, Y. Ohki, K. Sasagane, K. Nagasawa, Y. Hama, Phys. Rev. B 39 (1989) 1337.
[29] F.J. Fiegl, W.B. Fowler, K.L. Yip, Solid State Commun. 14 (1974) 225.
[30] M.E. Gimon-Kinsel, K. Groothuis, Kenneth J. Balkus, Micropor. Mesopor. Mater. 20 (1998) 67.
[31] M. Guzzi, M. Martini, F. Pio, G. Spinolo, A. Vedda, in: R.A.B. Devine (Ed.), The Physics ant Technology of Amorphous SiO$_2$, Plenum Press, New York, 1988, p. 175.
[32] N. He, S. Ge, C. Yang, M. Gu, Mater. Res. Bull. 39 (2004) 1931.